Synthesis and Electroluminescent Properties of High-Efficiency Saturated Red Emitter Based on Copolymers from Fluorene and 4,7-Di(4-hexylthien-2-yl)-2,1,3-benzothiadiazole

Qiong Hou, Qingmei Zhou, Yong Zhang, Wei Yang, Renqiang Yang, and Yong Cao*

Institute of Polymer Optoelectrionic Material and Devices, Key Laboratory of Specially Functional Materials and Advanced Manufacturing Technology, South China University of Technology, Guangzhou, China 510640

Received April 24, 2004; Revised Manuscript Received June 19, 2004

ABSTRACT: Novel soluble conjugated random copolymers are synthesized by palladium-catalyzed Suzuki coupling reaction from 9,9-dioctylfluorene (DOF) and 4,7-di(4-hexylthien-2-yl)-2,1,3-benzothiadiazole (DHTBT) with DHTBT composition varying from 1 to 50 mol % in the copolymer. All of the polymers are soluble in common organic solvents and are highly photoluminescent. Polyfluorene fluorescence is quenched completely at a DHTBT concentration as low as 1% in the solid film. The copolymer films are highly fluorescent under UV irradiation in contrast to its parent analogue, 4,7-di(thien-2-yl)-2,1,3-benzothiadiazole (PFO−DBT), without alkyl substitution on thiophene rings. Devices made up of these copolymers emit saturated red light. The emission peaks are shifted from 613 to 672 nm when the DHTBT content increases from 1 to 50%. The highest external quantum efficiency achieved in the device configuration ITO/PEDT/PVK/PFO−DHTBT/Ba/Al is 2.54% with luminous efficiency 1.45 cd/A for the copolymer with emission peak at 638 nm for 10% DHTBT content, among the highest values so far reported for saturated red polymer emitters.

Introduction

Recently, the commercial value of electroluminescent conjugated polymers have absorbed considerable interest due to their possible application in large area flat-panel displays[1] and other optoelectronic applications.[2,3] A wide range of conjugated polymers as the emissive layers such as poly(*p*-phenylenevinylene) (PPV) and their derivatives,[1,4−7] polythiophenes,[8,9] and polyfluorenes[10,11] have been developed and investigated in order to obtain stable high-efficiency RGB emitters. Among these conjugated polymers, polyfluorene (PFO) polymers and their derivatives have been studied since poly(9,9-di-*n*-hexylfluorene) (PDHF) was first reported as a blue-light-emitting polymer by Yoshino et al. in 1991.[12] Polyfluorene polymers and their derivatives have the advantages of a highly efficient fluorescence quantum yield, an excellent thermal and oxidative stability, and good solubility in common organic solvents.[13−15] As a result, these materials have emerged as a very promising candidate for polymer light-emitting diodes.[16,17] Emission color of polyfluorenes can be changed over an entire visible region by introducing narrow-band-gap comonomer into the polyfluorene backbone. Most widely used narrow-band-gap comonomers are a variety of aromatic heterocycles containing N or S atoms, such as thiophene,[18−21] benzothiadiazole,[17] and thiophene-containing heterocycles.[22−28] Compared with a high-efficiency green polyfluorene emitter based on copolymer from fluorene and benzothiadiazole, the high-efficiency polymer emitter with a saturated red emission remains a great challenge. Saturated red polyfluorene emitter was first synthesized by the Dow group reported in a patent literature probably by alternating copolymerization of fluorene and 4,7-dithienyl-2,1,3-benzothiadiazole (DBT).[29] The alternating copolymer of fluorene and qunquethiphene-1″,1″-dioxide with emission peak at around 666 nm and luminous efficiency 0.02 cd/A has been reported by the Leclerc group.[30,31] The Morgado group has reported similar results with an alternating copolymer from ethylhexylfluorene and 2,5-bis(2′-vinylthienyl)thiophene.[32] Significant enhancement in efficiency (up to 1.4%) with emission peak at 663 nm for PFO−DBT copolymer was recently reported by our group.[28] Cambridge Display Technology (CDT) announced a saturated red emitter with a high external quantum efficiency of 3% and a power efficiency of 1.2 lm/W with an emission peak at 650 nm, though the detailed chemical structure was not disclosed.[24] Recently, we also reported the syntheses and properties of a red emitter from fluorene and selen-containing heterocycle: 2,1,3-naphthoselenadiazole (NSeD) with a luminous efficiency about 0.9 cd/A and an emission peak at 657 nm.[25] As a summary of the results so far reported in the scientific literature, the luminous efficiency of a saturated emitter composed of fluorene and condensed thiophene-related heterocycles is around 1 cd/A. The results are not unexpected considering the low photoluminescence efficiencies of copolymers from fluorene and thiophene-related heterocycles in the solid state.[25,28]

In this paper we report the synthesis and characterization of the copolymers derived from fluorene with 4,7-di(4-hexylthien-2-yl)-2,1,3-benzothiadiazole (DHTBT) (structures in Scheme 1) in under or up to 50% (molar) in the polymer composition by the Suzuki coupling reaction. The alkyl side chain in the 4-position of both thiophene rings gives the material a good solubility. More important, the PL efficiency of such copolymers is significantly enhanced in the solid state in comparison with its unsubstituted analogue, PFO−DBT. Devices based on the copolymers emit a saturated red light. The highest quantum efficiency achieved in device configuration ITO/PEDT/PVK/PFO−DHTBT/Ba/Al was 2.54% for the copolymer with emission peak at 638 nm for 10%

* Corresponding author: Ph 86-020-87114609; Fax 86-020-87114535; e-mail poycao@scut.edu.cn.

10.1021/ma049204g CCC: $27.50
Published on Web 07/28/2004

Scheme 1. Synthesis Route of Comonomer and Copolymers

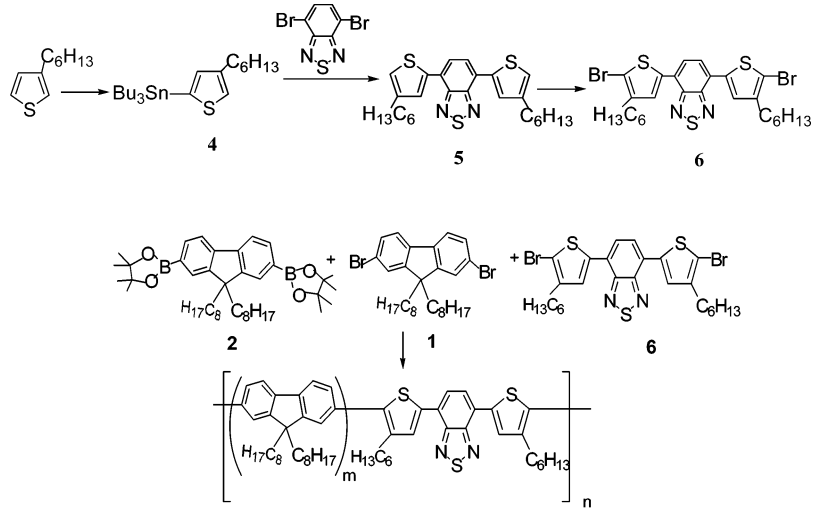

DHTBT content. The device performance (external quantum and luminous efficiencies) is almost doubled for a single-layer device as compared to that from its parent analogue, PFO−DBT, of the same composition without alkyl substitution at thiophene rings.

Experimental Section

Materials and Measurement. All reagents, unless otherwise specified, were purchased from Aldrich, TCI, and Acros and were used as they were received. All solvents were carefully dried and purified under a nitrogen flow. All manipulations involving air-sensitive reagents were performed in a dry argon atmosphere. ^{1}H and ^{13}C NMR spectra were recorded on Varian Inova 500 or Bruker DRX 400 in deuterated chloroform solution. Number-average (M_n) and weight-average (M_w) molecular weights were determined by a Waters GPC 2410 in tetrahydrofuran (THF) using a calibration curve of polystyrene standards. The elemental analysis was performed on Vario EL elemental analysis instrument (ELEMENTAR Co.). UV−vis absorption spectra were recorded on a HP 8453 spectrophotometer. Cyclic voltammetry were done by using a CHI660A electrochemical workstation with platinum electrodes at a scan rate of 50 mV/s against a calomel reference electrode with an anhydrous and nitrogen-saturated solution of 0.1 mol/L tetrabutylammonium hexafluorophosphate (Bu_4NPF_6) in acetonitrile (CH_3CN). The deposition of polymers on the electrode was done by the evaporation of a dilute chloroform solution. The PL quantum yields were determined in integrating sphere IS080 (Labsphere) with 405 nm excitation of UV diode laser (CL-2000, crystal laser). PL spectra were determined by Instaspec 4 CCD spectrophotometer (Oriel) uner of 325 nm line of the HeCd laser.

2,7-Dibromo-9,9-dioctylfluorene (**1**),[33] 2,7-bis(4,4,5,5-tetramethyl-1,3,2-dioxaborolan-2-yl)-9,9-dioctylfluorene (**2**),[33] and 4,7-dibromo-2,1,3-benzothiadiazole (**3**)[34] were prepared following the already published procedures.

4-(Hexyl-2-thienyl)stannane (4).[28,35] To a solution of 3-hexylthiophene in anhydrous THF at −30 °C, *n*-BuLi was added dropwise and the mixture was stirred at this temperature under N_2 for 2 h. Then tributylchlorostannane was added, and the mixture was stirred at −30 °C for 30 min. The mixture was poured into saturated aqueous sodium hydrogen carbonate, and the organic phase was separated and washed with saturated aqueous brine and then dried over an anhydrous sodium sulfate. The solvent was removed at a reduced pressure, and the residue was purified by column chromatography (neutral alumina, light petroleum) to give the product as colorless oil (yield: 73%).

4,7-Di(4-hexyl-2-thienyl)-2,1,3-benzothiadiazole (5).[28,36] $PdCl_2(PPh_3)_2$ was added to a solution of 4,7-dibromo-2,1,3-benzothiadiazole and tributyl-(4-hexyl-2-thienyl)stannane in THF. The mixture was refluxed in a nitrogen atmosphere for 6 h. After the removal of the solvent at a reduced pressure, the residue was purified by column chromatography on silica gel (eluent CH_2Cl_2/petroleum (60−90 °C, 1:1)). Recrystallization from ethanol gave the compound (yield: 88%) as orange needles; mp 76−78 °C. FAB-MS: 468. ^{1}H NMR (500 MHz, $CDCl_3$) δ (ppm): 7.97 (dd, 2H), 7.82 (s, 2H), 7.04 (dd, 2H), 2.66 (m, 4H), 1.70 (m, 4H), 1.25−1.53 (m, 12H), 0.90 (t, 6H). ^{13}C NMR (100 MHz, $CDCl_3$) δ (ppm): 126.15, 126.38, 127.21, 127.90, 128.42, 139.75, 153.02. Element Anal. Calcd for $C_{26}H_{32}N_2S_3$: C, 66.67%; H, 6.84%; N, 5.98%; S, 20.51%. Found: C, 66.30%; H, 6.94%; N, 5.99%; S, 20.82%.

4,7-Bis(5-bromo-4-hexyl-2-thienyl)-2,1,3-benzothiadiazole (6). 4,7-Di(4-hexyl-2-thienyl)-2,1,3-benzothiadiazole was added into THF in nitrogen flow. After the solid dissolved completely, *N*-bromosuccinimide (NBS) was added in one portion. The reaction mixture was stirred at a room temperature for 2 h, hexane was added into the mixture, the white precipitate formed was filtered off, the filtrate was extracted with ether, and the organic layer was washed with brine and dried over anhydrous sodium sulfate. The solvent was removed at a reduced pressure to give the product as a red solid (yield: 82%); mp 101−104 °C. FAB-MS: 626. ^{1}H NMR (500 MHz, $CDCl_3$) δ (ppm): 7.75 (s, 2H), 7.69 (s, 2H), 2.63 (m, 4H), 1.67 (m, 4H), 1.33−1.40 (m, 12H), 0.90 (t, 6H). ^{13}C NMR (100 MHz, $CDCl_3$) δ (ppm): 151.99, 142.98, 138.45, 127.94, 125.02, 124.51, 111.59, 31.68, 29.70, 29.03, 22.67, 14.14. Element Anal. Calcd for $C_{26}H_{30}N_2S_3Br_2$: C, 49.84%; H, 4.79%; N, 4.47%; S, 15.34%; Br, 25.26%. Found: C, 50.61%; H, 5.26%; N, 4.37%; S, 14.86%; Br, 24.9%.

Polymer Synthesis.[33] The synthesis of the copolymers was carried out using palladium-catalyzed Suzuki couplings. Carefully purified 2,7-dibromo-9,9-dioctylfluorene (**1**), 2,7-bis(4,4,5,5-tetramethyl-1,3,2-dioxaborolan-2-yl)-9,9-dioctylfluorene (**2**), 4,7-bis(5-bromo-4-hexyl-2-thienyl)-2,1,3-benzothiadiazole (DHTBT) (**6**), and $(PPh_3)_4Pd(0)$ (0.5−1.5 mol %) and several of drops Aliquat336 were dissolved in a mixture of toluene and aqueous solution of 2 M Na_2CO_3. The mixture was first put in the argon atmosphere and was refluxed with vigorous stirring for 48 h. Then 2,7-dibromo-9,9-dioctylfluorene and 2-(4,4,5,5-tetramethyl-1,3,2-dioxaborolan-2-yl)-9,9-dioctylfluorene were added to end-cap the polymer chain. The whole mixture was poured

into methanol. The resulted solid was filtered and washed with acetone to remove oligomers and catalyst residues. Yield: 76%−85%. The resulted polymers were soluble in conventional organic solvents (toluene, chloroform, and tetrahydrofuran). The results of elemental analyses of sulfur and carbon for each copolymer were used for the calculation of actual copolymer composition. Element Anal. Found: for PFO−DHTBT1: C, 88.73%; S, 0.66%; for PFO−DHTBT5: C, 87.30%; S, 1.24%; for PFO−DHTBT10: C, 86.20%; S, 2.32%; for PFO−DHTBT15: C, 84.52%; S, 3.38%; for PFO−DHTBT25: C, 80.84%; S, 5.56%; for PFO-DHTBT35: C, 77.94%; S, 8.30%; for PFO−DHTBT50: C, 77.14%; S, 10.92%.

NMR results: for PFO−DHTBT50: ^{1}H NMR (500 MHz, $CDCl_3$) δ (ppm): 8.07 (s, 2H), 7.89 (s, 2H), 7.77 (d, 2H), 7.53 (s, 4H), 2.81 (s, 4H), 2.06 (s, 4H), 1.75 (s, 4H), 1.53 (s, 4H), 1.13−1.40 (m, 32H), 0.79−0.89 (m, 12H). ^{13}C NMR (100 MHz, $CDCl_3$) δ (ppm): 152.74, 151.34, 140.38, 139.89, 137.70, 137.15, 133.35, 130.46, 128.25, 125.79, 125.28, 123.60, 119.94, 118.99, 55.31, 43.13, 31.81, 31.12, 30.16, 29.36, 24.05, 22.66, 14.07.

LED Fabrication and Characterization. Polymers were dissolved in *p*-xylene and filtered through a 0.45 μm filter. Patterned indium tin oxide (ITO)-coated glass substrates were cleaned with acetone, detergent, distilled water, and 2-propanol, subsequently in an ultrasonic bath. After treatment with oxygen plasma, 150 nm of poly(3,4-ethylenedioxythiophene) (PEDOT) doped with poly(styrenesulfonic acid) (PSS) (Batron-P 4083, Bayer AG) was spin-coated onto the ITO substrate followed by drying in a vacuum oven at 80 °C for 8 h. For some devices, poly(vinylcarbazole) (PVK, Aldrich) from 1,1,2,2-tetrachloroethane solution was coated on top of a dried PEDOT−PSS layer subsequently. A thin film of electroluminescent polymer was coated onto the anode by spin-casting inside a drybox. The film thickness of the active layers was around 70 nm, as measured with an Alfa Step 500 surface profiler (Tencor). We note that since PVK is not soluble in *p*-xylene, PVK remains untouched during spinning top DHTBT layer. A thin layer of Ba (4−5 nm) and subsequently 200 nm layers of Al were vacuum-evaporated subsequently on the top of an EL polymer layer under a vacuum of 1×10^{-4} Pa. Device performances were measured inside a drybox. Current−voltage (I−V) characteristics were recorded with a Keithley 236 source meter. EL spectra were recorded by Oriel Instaspec IV CCD spectrograph. Luminance was measured by a PR 705 photometer (Photo Research). The external quantum efficiencies were determined by a Si photodiode with calibration in an integrating sphere (IS080, Labsphere).

Results and Discussion

Synthesis and Characterization of Copolymers. The general synthetic routes toward the monomers and polymers are outlined in Scheme 1. Monomer **5** was synthesized via Stille coupling method from monomer **3** and monomer **4**. Monomer **6** was prepared from monomer **5** and NBS in THF. To the best of our knowledge, monomer **6**, 4,7-bis(5-bromo-4-hexyl-2-thienyl)-2,1,3-benzothiadiazole, is synthesized for the first time.

Through the synthetic route in Scheme 1, conjugated copolymers of different compositions were prepared from 2,7-dibromo-9,9-dioctylfluorene (DOF), 2,7-bis(4,4,5,5-tetramethyl-1,3,2-dioxaborolan-2-yl)-9,9-dioctylfluorene, and narrow-band-gap comonomer 4,7-bis(5-bromo-4-hexyl-2-thienyl)-2,1,3-benzothiadiazole (DHTBT) using palladium-catalyzed Suzuki coupling methods. The comonomer feed molar ratios of DOF to DHTBT are 99:1, 95:5, 90:10, 85:15, 75:25,65:35, and 50:50, respectively, and the corresponding copolymers were named PFO−DHTBT1, PFO−DHTBT5, PFO−DHTBT10, PFO−DHTBT15, PFO−DHTBT25, PFO−DHTBT35, and PFO−DHTBT50, respectively. For these copolymers, *n*-octyl substituents in the 9-position of fluorene and *n*-hexyl substituents in the 4-position of thiophene were employed to improve the solubility of the resulted

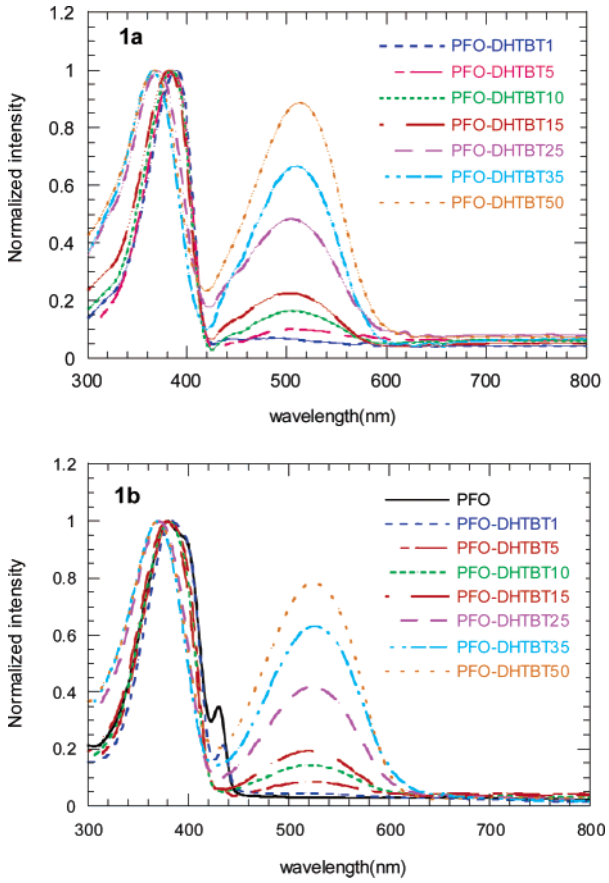

Figure 1. (a) UV−vis absorption spectra for the copolymers in $CHCl_3$ solution. (b) UV−vis absorption spectra for the copolymers in thin film.

Table 1. Molecular Weights of the Copolymers and Copolymer Composition Determined by Elemental Analysis

			DOF/DHTBT	
copolymers	M_n ($\times 10^3$)	M_w/M_n	in the feed composition	in the copolymers[a]
PFO−DHTBT1	16	2.7	99/1	97.3/2.7
PFO−DHTBT5	15	2.5	95/5	94.9/5.1
PFO−DHTBT10	67	2.9	90/10	90.3/9.7
PFO−DHTBT15	18	2.3	85/15	85.7/14.3
PFO−DHTBT25	3	2.0	75/25	75.7/24.3
PFO−DHTBT35	4	1.9	65/35	62.9/37.1
PFO−DHTBT50	40	2.1	50/50	51.3/48.7

[a] Calculated from results of elemental analysis.

copolymers. At the end of polymerization, 2,7-dibromo-9,9-dioctylfluorene was added to remove boronic acid ester end groups, 2-(4,4,5,5-tetramethyl-1,3,2-dioxaborolan-2-yl)-9,9-dioctylfluorene, as a monofunctional end-capping reagent was added to remove bromine end groups because boron and bromine units could quench emission and contribute to red shift of EL emission in PLEDs.[37,38] The starting monomer molar ratios have been adjusted in order to investigate the effect of copolymer composition on the physical and optical properties. The actual molar ratio of DOF/DHTBT in the copolymer calculated from elemental analysis is very close to the feed ratio as listed in Table 1. Incorporation of DHTBT into the polyfluorene main chain was also monitored by UV spectroscopy (λ_{max}(oligofluorene segments) = 380 nm, λ_{max}(incorporated DHTBT) = 520 nm) (Figure 1). The number-average molecule weights (M_n) of the synthesized copolymers, PFO−DHTBT1 to PFO−

Table 2. UV−vis Properties and Electrochemical Properties of the Copolymers

copolymers	$\lambda_{abs,max}$/nm	optical band gap[a]/eV for DOF segment	optical band gap[a]/eV for DHTBT unit	E_{ox}/V	HOMO/eV	LUMO[b]/eV
PFO−DHTBT1	383	2.91		1.36	−5.76	2.85
PFO−DHTBT5	382, 520	2.94	2.09	1.28	−5.68	−3.59
PFO−DHTBT10	381, 520	2.91	2.07	1.38,1.28	−5.68	−3.61
PFO−DHTBT15	378, 520	2.94	2.06	1.35,1.24	−5.64	−3.58
PFO−DHTBT25	371, 522	2.95	2.06	1.38,1.22	−5.62	−3.56
PFO−DHTBT35	369, 526	2.94	2.03	1.36,1.22	−5.62	−3.59
PFO−DHTBT50	370, 525	2.94	2.06	1.35, 1.20	−5.60	−3.54

[a] Estimated from the onset wavelength of optical absorption in solid film. [b] Calculated from HOMO level and the onset of optical absorption of DHTBT unit.

DHTBT50, were determined by gel permeation chromatography (GPC) using a polystyrene standard (Table 1). A polydispersity index (M_w/M_n) was around 19−2.9 (Table 1), typical for a polycondensation reaction. As shown in Scheme 1, the particular advantage of polymerization by Suzuki coupling is that each individual narrow-band-gap unit is separated from both sides by wide-band-gap segments for copolymers with the narrow-band-gap component under or equal to 50 mol % in the copolymer. In this case we could expect the narrow-band-gap unit functions as an exciton trap which allows most efficient intramolecular energy transfer from fluorene segment to DHTBT unit as shown in other random copolymers synthesized via Suzuki coupling.[25,28,39]

Optical and Electrochemical Properties. The absorption spectra of polymers PFO−DHTBT in $CHCl_3$ solution and in solid state are shown in parts a and b of Figure 1, respectively. All the copolymers showed similar absorption spectra in the solution (Figure 1a) and in the solid films (Figure 1b). The absorption spectra of the copolymers measured in thin films consist of two absorption peaks both in the solution and in solid states. The absorption peak appeared at ca. 380 nm in the solid films and is consistent with those reported for poly(9,9-dihexylfluorene) homopolymer (388 nm).[40] This peak can be attributed to the fluorene segment in the copolymer. An extralong wavelength absorption band at ca. 520 nm, the intensity of which increases with increasing of DHTBT content, can be attributed to the DHTBT unit incorporated into the polyfluorene main chain. In the case of the copolymer containing 1% of DHTBT in the copolymer, the presence of the DHTBT unit is not apparent from the absorption spectrum in the solid film (Figure 1b). However, a weak 520 nm peak is clearly seen in the solution spectrum of 1% DHTBT copolymer (Figure 1a).

The electrochemical properties of the copolymers were investigated by cyclic voltammetry (CV) in order to gauge their electronic properties. All the electrochemical data for PFO−DHTBT obtained from the films are listed in Table 2. Except the copolymers with 1% and 5% DHTBT, we can record two p-doping waves. However, we failed to detect n-doping process in these copolymers. For copolymers with DHTBT content equal to or over 10%, the first onset of p-doping wave decreases with the increasing of DHTBT content from 1.28 V for PFO−DHTBT10 to 1.20 V for PFO−DHTBT50. The second onset of oxidation process is almost constant for all copolymers at about 1.35−1.38 V. Since the oxidation potential for polyfluorene homopolymer was observed typically at 1.4 V,[41] the second oxidation wave can be assigned to the oxidation process for the fluorene segments in the copolymers. The first oxidation wave observed at 1.20−1.28 V in the copolymers must be attributed to the oxidation process for the DHTBT unit. For PFO−DHTBT1 only one peak can be observed in the voltammogram. The position of the onset of this peak is the same (1.36 V) as the second onset (DOF segments) in copolymer with high DHTBT content. HOMO level is calculated according to the empirical formula ($E_{HOMO} = -e(E_{ox} + 4.4$ eV).[42] LUMO level is estimated from the optical band gap. HOMO and LUMO levels are listed in Table 2. HOMO levels responsible for DHTBT unit slightly decreases with the increasing of DHTBT content and becomes 5.60 eV for PFO−DHTBT50. Keep in mind that a single DHTBT unit is isolated from both sides by fluorene segments, and the change in HOMO levels for DHTBT units must be originated from interchain interaction. Two well-defined oxidation processes in the cyclic voltammograms and the similarity of the onset of oxidation waves for DOF segment in the copolymers and homopolymer demonstrate again that the electronic states of both components, DOF and DHTBT, in the copolymers are not mixed. This is consistent very well with the two separated absorption peaks in the UV−vis spectra (Figure 1).

Photoluminescent Properties. Parts a and b of Figure 2 show the photoluminescent (PL) spectra of the polymers PFO−DHTBT by the excitation of the 325 nm line of the HeCd laser in $CHCl_3$ solution and in thin film, respectively. In the thin solid film, polyfluorene emission was completely quenched, and PL emission consists exclusively of DHTBT emission at DHTBT concentration as low as 1% (Figure 2b). PL emission peaks are gradually red-shifted with the increasing of DHTBT content in the copolymers, from 629 nm for the copolymer PFO−DHTBT1 to 669 nm for the alternating copolymer PFO−DHTBT50. In the $CHCl_3$ solution (Figure 2a) with the copolymer concentration of 1×10^{-5} mol/L (by repeat unit), excluding copolymer PFO−DHTBT50, all the copolymers show two PL emission consisting of two emission features peaked at around 420 and 655 nm. An intensity of the emission at around 420 nm decreases with the increasing of DHTBT content in the copolymers while the intensity of the red-emitting peak increases with the increasing of DHTBT content. Therefore, 420 nm emission can be assigned to the emission of DOF segment in the copolymer, and 655 nm emission can be assigned to the emission of DHTBT unit (Figure 2a). For copolymers with DHTBT content equal to or over 5%, the PL emission is dominated by DHTBT unit, and an emission from the PFO segments gradually decreases with the increase of the DHTBT content. Figure 3a shows the concentration dependence of PL profile of PFO−DHTBT1 (1% DHTBT in copolymer) in $CHCl_3$ solution. With the increasing of the DHTBT1 concentration in the solution, the intensity of 420 nm peak (responsible for DOF emission) decreases while the

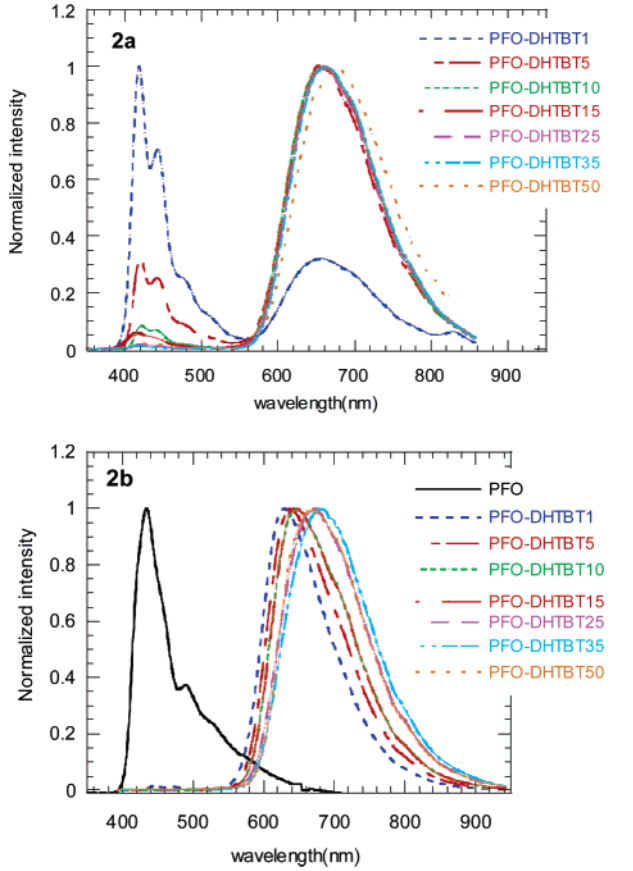

Figure 2. (a) PL spectra of the copolymers in the $CHCl_3$ solution in the concentration of 1×10^{-5} mol/L under 325 nm excitation. (b) PL spectra of the copolymers in thin film under 325 nm excitation.

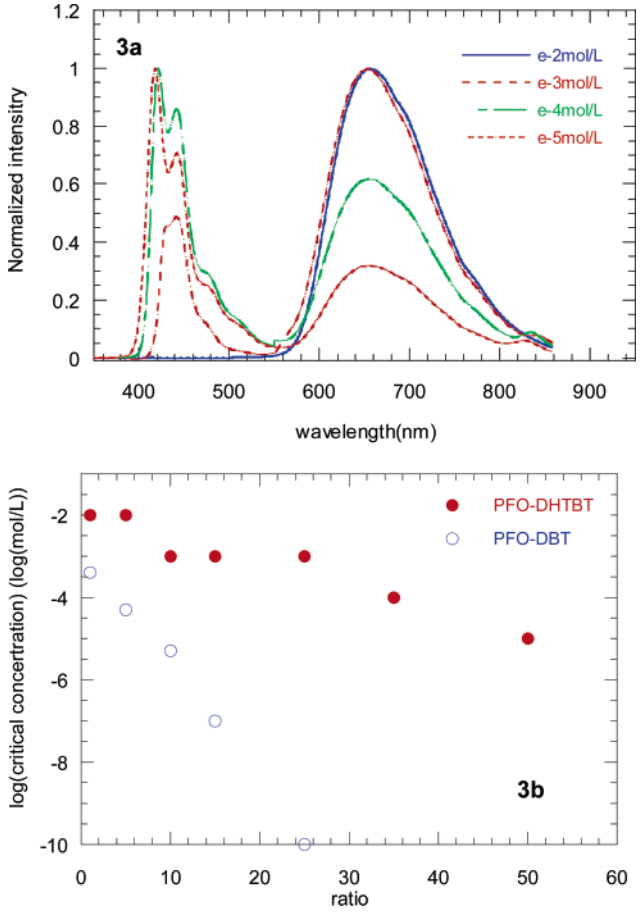

Figure 3. (a) Concentration dependence of PL profile of PFO−DHTBT1 (1% DHTBT in copolymer) in $CHCl_3$ solution. (b) Critical concentration (in log scale) as a function of molar ratio of DHTBT in the copolymers.

655 nm peak increases. Polyfluorene emission was completely quenched when the concentration of PFO−DHTBT1 is equal to or greater than 1×10^{-2} mol/L (Figure 3a). We define a concentration at which polyfluorene fluorescence (420 nm) was completely quenched as a critical concentration in the copolymer solution (determined practically as a concentration at which PL emission at 420 nm with intensity plotted in a logarithm scale is completely disappeared). Figure 3b shows the curve of critical concentration (in log scale) vs molar ratio of DHTBT comonomer in the copolymer in the solution. The critical concentration of PFO−DHTBT decreases gently with the increasing of the DHTBT content in the copolymers in the solution from 10^{-2} mol/L for PFO−DHTBT1 to 10^{-5} mol/L for PFO−DHTBT50. For comparison, in Figure 3b we also included critical concentration vs DBT content for PFO−DBT copolymers which has no alkyl substitution in the thiophene rings.[28] As can be seen from Figure 3b, the critical concentration of PFO−DBT copolymers shows significantly larger dependence on the molar ratio of narrow-band-gap component. This fact indicates that the alkyl substitution on the thiophene rings in DHTBT greatly reduces the interchain interaction of PFO−DHTBT copolymers in comparison with that of PFO−DBT. We have reported previously that PFO−DBT copolymers shows very low PL efficiency in the solid state films, and the PL efficiency decreases very quickly with the increasing of DBT content (Table 3).[28] This fact was thought to be the results of increasing interchain interaction with the increase of DBT content in the copolymers.[28] It is suggested that interchain interaction

Table 3. PL Emission Peak and PL Efficiency of PFO−DHTBT (in Comparison with PFO−DBT) Thin Solid Films

	photoluminescence			photoluminescence	
copolymers	$\lambda_{Pl,max}$/nm	QE_{PL} (%)[a]	copolymers	$\lambda_{Pl,max}$/nm	QE_{PL} (%)[b]
PFO−DHTBT1	629	88.2	PFO−DBT1	635	11.4
PFO−DHTBT5	636	74.6	PFO−DBT5	651	12.5
PFO−DHTBT10	647	68.6	PFO−DBT10	655	8.6
PFO−DHTBT15	642	69.6	PFO−DBT15	678	7.9
PFO−DHTBT25	670	50.4	PFO−DBT25	678	5.2
PFO−DHTBT35	678	43.8	PFO−DBT35	685	4
PFO−DHTBT50	669	19.0			

[a] Obtained under 405 nm excitation. [b] Obtained under 325 nm excitation.

should be significantly reduced for PFO−DHTBT due to alkyl substitution on thiophene rings in comparison with its parent analogue, PFO−DBT. As a result, we can expect that PFO−DHTBT copolymer might have the enhanced PL efficiency in the solid state. Table 3 lists the PL efficiencies obtained with 405 nm excitation. To make a comparison, PL efficiency of PFO−DBT[28] is listed in Table 3, too. Copolymers of PFO−DHTBT have much higher PL efficiency in the solid film than those of PFO−DBT copolymers. This fact indicates that the introduction of the long alkyl chain into the thiophene ring prevents a close packing of polymer chains and thereby reduces significantly concentration quenching due to the interchain interaction in PFO−DHTBT copolymers. The fact that PL emission of PFO−DHTBT

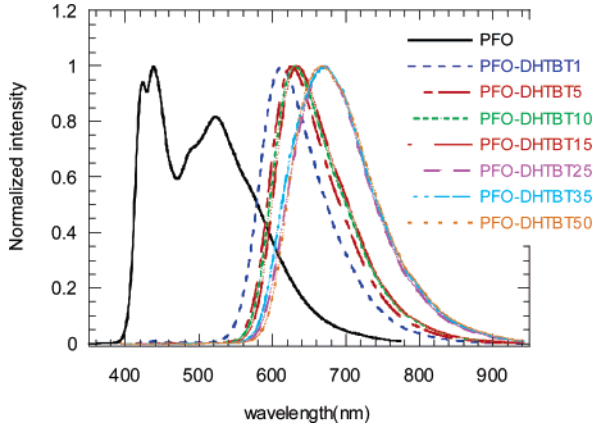

Figure 4. EL spectra of devices from the copolymers.

Table 4. Device Performance of PFO−DHTBT Copolymers in Device Configuration: ITO/PEDT/PFO−DHTBT/Ba/Al

	device performance						chromaticity coordinates	
copolymers	$\lambda_{El,max}$/ nm	V	mA cm^{-2}	cd m^{-2}	cd/A	Q_{ext}/ %	*x*	*y*
PFO−DHTBT1	613	8.5	22.7	84.6	0.37	0.65	0.60	0.38
PFO−DHTBT5	625	8.0	25.1	146.9	0.58	1.02	0.65	0.35
PFO−DHTBT10	629	5.5	41.1	257.5	0.63	1.10	0.66	0.34
PFO−DHTBT15	634	5.0	42.3	350.9	0.83	1.45	0.66	0.34
PFO−DHTBT25	672	4.0	34.3	43.2	0.13	0.42	0.67	0.33
PFO−DHTBT35	671	3.5	28.3	26.0	0.09	0.31	0.68	0.32
PFO−DHTBT50	669	4.5	26.3	19.7	0.08	0.25	0.68	0.32

is around 5−10 nm blue-shifted (Table 3) than that of PFO−DBT copolymers of same composition indicates also less interchain interaction in the PFO−DHTBT copolymers. We note that PL efficiency of PFO−DHTBT decreases with the increasing of the DHTBT content in the copolymers from 88% for PFO−DHTBT1 to around 19% for PFO−DHTBT50. Like DBT in PFO−DBT copolymer, the DHTBT unit in the PFO−DHTBT copolymer serves as a quenching channel (both radiative and nonradiative) in these copolymers. The PL efficiency measurement is consistent well with the dependence of the critical concentration on DHTBT content shown in Figure 3b.

Electroluminescent Properties. The EL performance of the copolymers was examined in the device configuration of ITO/PEDT/PFO−DHTBT/Ba/Al and ITO/PEDT/PVK/PFO−DHTBT/Ba/Al. The typical EL spectra from such device are shown in Figure 4. The EL spectrum of polyfluorene homopolymer is also shown in Figure 4 for comparison. We note that due to the introduction of a small amount of (from DHTBT content 1%) of DHTBT into polyfluorene chain, PFO emission at around 430 nm and a broad excimer emission[43] peaked at around 530 nm observed typically for polyfluorenene homopolymers are completely quenched (Figure 4). We note that recently several groups attributed this long wavelength emission shoulder to the fluorenone defects introduced by photooxidation and thermal oxidization.[44−46] For devices fabricated from PFO−DHTBT copolymers of all compositions, starting from DHTBT content as low as 1%, only a saturated red emission responsible for DHTBT unit has been observed. This fact indicates that energy transfer from DOF segment to DHTBT unit is very efficient and quick process which suppress both radiative decay from DOF segment and excimer emission. EL peaks are generally 10 nm blue-shifted (Figures 2 and 4) in comparison with

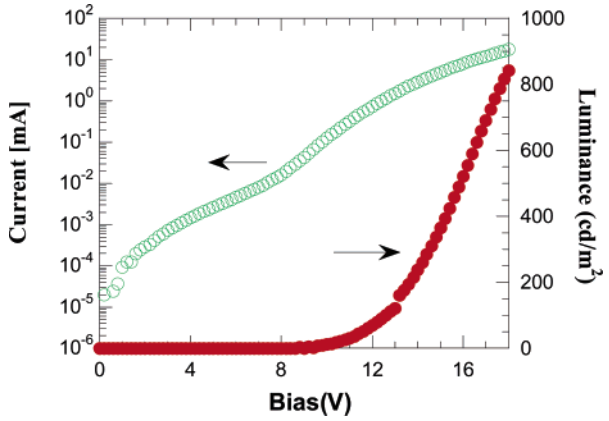

Figure 5. Current−voltage and luminance−voltage curve of copolymers PFO−DHTBT10 with device structure of ITO/PEDT/PVK/PFO−DHTBT/Ba/Al.

Table 5. Device Performance from PFO−DHTBT Copolymer with PVK as an Anode Buffer (in Device Configuration: ITO/PEDT/PVK/ PFO−DHTBT/Ba/Al)

	device performance						chromaticity coordinates	
copolymers	$\lambda_{Els,max}$/ nm	V	mA cm^{-2}	cd m^{-2}	Cd/A	Q_{ext}/ %	*x*	*y*
PFO−DHTBT5	634	15.0	33.3	366	1.1	1.93	0.66	0.34
PFO−DHTBT10	638	10.6	28.5	413	1.45	2.54	0.66	0.34
PFO−DHTBT15	647	9.6	32.8	392	1.19	2.09	0.67	0.33

the PL emission of corresponding copolymers. EL peaks are also red-shifted with the increasing of DHTBT content as in PL emission. EL emission peaks are shifting from 613 nm for PFO−DHTBT1 to 669 nm for PFO−DHTBT50 (Figure 4 and Table 4). The chromaticity coordinates changed from $x = 0.60$, $y = 0.38$ for PFO−DHTBT1 to $x = 0.68$, $y = 0.32$ for PFO−DHTBT50 (Table 4). The great red shift in EL emission with the increase in DHTBT content indicates an aggregation between DHTBT units of neighboring chains. For small molecule dye-doped polymer LEDs, it is typically observed a big difference between PL and EL spectra at a low doping concentration region, for example for devices fabricated with blend films from Eu complex/CNPPP,[44] PtOEP/PFO,[45] and Ir complex doped PFO and PVK.[46] For these systems host PL emissions were quenched completely only at a doping concentration of ≥4−8%, much higher than the doping concentration of 1−2%, at which the host EL emission is completely quenched. For copolymers mentioned in this paper, the host emission has been quenched at DHTBT content as low as 1% for both PL and EL emission. This fact seems to indicate that, in contrast to the dye-doped polymer system where energy transfer is intermolecular, the energy transfer of PFO−DHTBT copolymers occurred mainly within polymer chain via intramolecular trapping mechanism along conjugated polymer chain. As a result, for copolymers PFO−DHTBT, the generated excitons are efficiently confined on the DHTBT site, copolymers emit exclusively emission of the narrow-band-gap component, DHTBT.

Preliminary device data are promising. The external EL efficiencies in our standard device configuration ITO/PEDT/PFO−DHBT/Ba/Al with PEDT intralayer vary with copolymer compositions. The device performance is presented in Table 4. The external quantum efficiencies increase initially with the DHTBT content, reaching the maximum for copolymer with 15% DHTBT content, and then gradually decrease. The highest external EL

quantum efficiency in such a device configuration was 1.45%, and the luminous efficiency was 0.83 cd/A at the luminance of 351 cd/m^2 for copolymer with PFO−DHTBT15. As indicated by the CV measurement, the HOMO level of PFO−DHTBT copolymers is located around 5.6 eV toward vacuum level. Since PEDT has work function around 5.0−5.2 eV, there is expected a significant barrier for hole injection for the device configuration with PEDOT anode interlayer. To make improvement in hole injection, a thin PVK layer was coated on the top of PEDT prior to EL polymer coating. Table 5 shows device performance for several PFO−DHTBT copolymers with PVK interlayer. The $I-V$ and $L-V$ characteristics of device with PFO−DHTBT10 copolymer are shown in Figure 5. The results indicate that an insertion of PVK layer significantly enhances the device performance. The external quantum luminous efficiencies reached 2.54% and l.45 cd/A for devices from copolymer PFO−DHTBT10, among the highest so far reported for a saturated red emitter.

Conclusions

We synthesized a series of new conjugated copolymers PFO−DHTBT, composed of random or alternating 9,9-dioctylfluorene and DHTBT, via a palladium-catalyzed Suzuki coupling reaction. All the obtained copolymers have excellent solubility in common organic solvents, such as $CHCl_3$, THF, and toluene. The efficient energy transfer due to exciton trapping on narrow-band-gap DHTBT sites has been observed. PL emission from fluorene segments was completely quenched at DHTBT concentration as low as 1% in the solid-state film. The copolymers are highly fluorescent at 620−660 nm under UV irradiation. A double-layer LED device with these polymers as the emitting layer shows a saturated red emission. The highest external quantum efficiency, 2.54%, and luminous efficiency, 1.45 cd/A, which peaked at around 630 nm are reached for the device fabricated with copolymer of 10% DHTBT content. This is among the highest values so far reported for saturated red polymer emitters.

Acknowledgment. This work was supported by Ministry of Science and Technology (#2002CB 613402) and the Natural Science Foundation of China (#50028302, # 90201023).

References and Notes

(1) Burroughes, J. H.; Bradley, D. D. C.; Brown, A. R.; et al. *Nature (London)* **1990**, *347*, 539.
(2) Wohrle, D.; Meissner, D. *Adv. Mater.* **1991**, *3*, 129.
(3) Lovinger, A. J.; Rothverg, L. J. *J. Mater. Res.* **1996**, *11*, 1581.
(4) Gustassion, G.; Cao, Y.; Treacy, G. M.; Klavetter, F.; Colaneri, N.; Heeger, A. J. *Nature (London)* **1992**, *357*, 477.
(5) Greenham, N. C.; Moratti, S. C.; Bradley, D. D. C.; Friend, R. H.; Burn, P. L.; Holmes, A. B. *Nature (London)* **1993**, *365*, 628.
(6) Son, S.; Dodabalapur, A.; Lovinger, A. J.; Galvin, M. E. *Science* **1995**, *269*, 376.
(7) Johansson, D. M.; Srdanov, G.; Yu, G.; Theaneder, M.; Inganas, O.; Anderson, M. R. *Macromolecules* **2000**, *33*, 2525−2529.
(8) Berggren, M.; Inganas, O.; Gustafsson, G.; Rasmusson, J.; Andersson, M. R.; Hjertberg, T.; Wemerstrom, O. *Nature (London)* **1994**, *372*, 444.
(9) Pei, J.; Yu, W. L.; Ni, J.; Lai, Y. H.; Huang, W.; Heeger, A. J. *Macromolecules* **2001**, *34*, 7241−7248.
(10) Fukuda, M.; Sawada, K.; Yoshino, K. *J. Polym. Sci., Part A: Polym. Chem.* **1993**, *31*, 2465−2471.
(11) Scherf, U.; W. List, E. J. *Adv. Mater.* **2002**, *14*, 477−487.
(12) Ohmori, Y.; Uchida, M.; Muro, K.; Yoshino, K. *Jpn. J. Appl. Phys.* **1991**, *30*, L1941−L1943.
(13) Pei, Q.; Yang, Y. *J. Am. Chem. Soc.* **1996**, *188*, 7416.
(14) Grell, M.; Long, X.; Bradley, D. D. C.; Inbasekaran, M.; Woo, E. P. *Adv. Mater.* **1997**, *9*, 798.
(15) Leclerc, M. *J. Polym. Sci., Part A: Polym. Chem.* **2001**, *39*, 2867.
(16) Inbasekaran, M.; Woo, E.; Wu, W. S.; Bernius, M.; Wujkowski, L. *Synth. Met.* **2000**, *111−112*, 397−401.
(17) Inbasekaran, M.; Woo, E. P.; Wu, W. S.; Bernius, M. T. PCT application W0046321A1, 2000.
(18) Larmat, F.; Reynolds, J. R.; Reinhardt, B. A.; Brott, L. L.; Clarson, S. J. *J. Polym. Sci., Part A: Polym. Chem.* **1997**, *35*, 3627−3636.
(19) Blondin, P.; Bouchard, J.; Beaupré, S.; Belletête, M.; Durocher, G.; Leclerc, M. *Macromolecules* **2000**, *33*, 5874−5879.
(20) Lévesque, I.; Donat-Bouillud, A.; Tao, Y.; D'Iorio, M.; Beaupré, S.; Blondin, P.; Ranger, M.; Bouchard, J.; Leclerc, M. *Synth. Met.* **2001**, *122*, 79−81.
(21) Charas, A.; Barbagallo, N.; Morgado, J.; Alcácer, L. *Synth. Met.* **2001**, *122*, 23−25.
(22) Bernius, M.; Inbasekaran, M.; Woo, E.; Wu, W. S.; Wujkowski, L. *J. Mater. Sci.: Mater. Electron.* **2000**, *11*, 111−116.
(23) Whitehead, K. S.; Grell, M.; Bradley, D. D. C.; Inbasekaran, M.; Woo, E. P. *Synth. Met.* **2000**, *111−112*, 181−185.
(24) Millard, I. S. *Synth. Met.* **2000**, *111−112*, 119−123.
(25) Yang, J.; Jiang, C. Y.; Zhang, Y.; Yang, R. Q.; Yang, W.; Hou, Q.; Cao, Y. *Macromolecules* **2004**, *37*, 1211−1218.
(26) Huang, J.; Xu, Y. S.; Hou, Q.; Yang, W.; Yuan, M.; Cao, Y. *Macromol. Rapid Commun.* **2002**, *23*, 709−712.
(27) Huang, J.; Niu, Y. H.; Yang, W.; Mo, Y. Q.; Yuan, M.; Cao, Y. *Macromolecules* **2002**, *35*, 6080−6082.
(28) Hou, Q.; Xu, Y. S.; Yang, W.; Yuan, M.; Peng, J. B.; Cao, Y. *J. Mater. Chem.* **2002**, *12*, 2887−2892.
(29) Woo, E. P.; Inbasekaran, M.; Shiang, W.; Roof, G. R. WO 99 05184, 1997.
(30) Beaupre, S.; Leclerc, M. *Adv. Funct. Mater.* **2002**, *12*, 192−196.
(31) Drolet, N.; Beaupre, S.; Morin, J.-F.; Tao, Y.; Leclerc, M. *J. Opt. A: Pure Appl. Opt.* **2002**, *4*, S252−S257.
(32) Charas, A.; Morgado, J.; Martinho, J. M. G.; Alcácer, L.; Cacialli, F. *Synth. Met.* **2002**, *127*, 215−254.
(33) Ranger, M.; Rondeau, D.; Leclerc, M. *Macromolecules* **1997**, *30*, 7686−7691.
(34) Pilgram, K.; Zupan, M.; Skile, R. *J. Heterocycl. Chem.* **1970**, *6*, 629.
(35) Pinhey, J. T.; Roche, E. G. *J. Chem. Soc., Perkin, Trans. 1* **1988**, 2415−2421.
(36) Kitamura, C.; Tanaka, S.; Yamashita, Y. *Chem. Mater.* **1996**, *8*, 570−578.
(37) Inbasekaran, M.; Wu, W.; Woo, E. P. United States Patent 5777070, 1998.
(38) Yang, X. H.; Yang, W.; Yuan, M.; Hou, Q.; Huang, J.; Zeng, X. R.; Cao, Y. *Synth. Met.* **2003**, *135−136*, 189−190.
(39) Yang, R. Q.; Tian, R. Y.; Hou, Q.; Yang, W.; Cao, Y. *Macromolecules* **2003**, *36*, 7453−7460.
(40) Kreyenschmidt, M.; Klaerner, G.; Fuhrer, T.; Ashenhurst, J.; Karg, S.; Chen, W. D.; Lee, V. Y.; Scott, J. C.; Miller, R. D. *Macromolecules* **1998**, *31*, 1099−1103.
(41) Janietz, S.; Bradley, D. D. C.; Grell, M.; Giebeler, C.; Inbasekaran, M.; Woo, E. P. *Appl. Phy. Lett.* **1998**, *73*, 2453−2455.
(42) Leeuw, D. M.; Simenon, M. M. J.; Brown, A. R.; Einerhand, R. E. F. *Synth. Met.* **1997**, *87*, 53.
(43) Lee, J.-I.; Klaerner, G.; Miller, R. D. *Chem. Mater.* **1999**, *11*, 1083−1088. Klärner, G.; Davey, M. H.; Chen, W.-D.; Scott, J. C.; Miller, R. D. *Adv. Mater.* **1998**, *10*, 993. List, E. J. W.; Guentner, R.; de Freitas, P. S.; Scherf, U. *Adv. Mater.* **2002**, *14*, 374−378. Herz, L. M.; Pillips, R. T. *Phys. Rev. B* **2000**, *61*, 13691.
(44) McGehee, M. D.; Bergstedt, T. T.; Zhang, C.; Saab, A. P.; O'Regan, M. B.; Bazan, G. C.; Srdanov, V. I.; Heeger, A. J. *Adv. Mater.* **1999**, *11*, 1349.
(45) O'Brien, D. F.; Giebeler, C.; Fletcher, R. B.; Cadby, A. J.; Palilis, L. C.; Lidzey, D. G.; Lane, P. A.; Bradley, D. D. C.; Blau, W. *Synth. Met.* **2001**, *116*, 379−383.
(46) Niu, Y. H.; Huang, J.; Cao, Y. *Adv. Mater.* **2003**, *15*, 807−811.

MA049204G